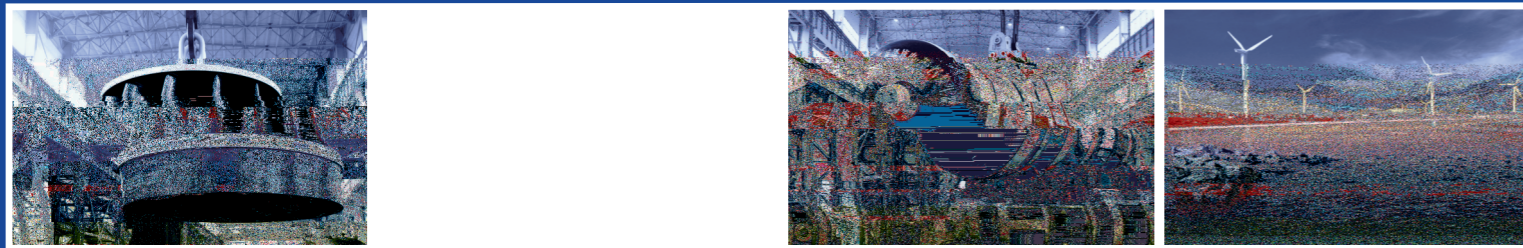


# DONGFANG ELECTRIC REVIEW



# 東方電氣評論

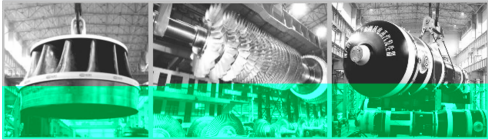
- 
- 
- 
- 
- 
-

2

2025

39 2 156  
1987

# 东方电气评论



质子交换膜燃料电池 ..... 李敏 胡小勇 张媛(1)

TOPCon 电池 ..... 杨隽 朱健 张乾 (8)

..... 李 (12)

..... 李 (18)

..... (22)

..... 李 杨 (28)

PLM 料 ..... (33)

300 Mvar ..... 李 (38)

Workbench ..... (44)

小 ..... (44)

..... (50)

..... (54)

..... (63)

..... 健 (68)

..... (73)

PLC ..... 张 (78)

UPS ..... (81)

..... (86)

..... (43)(67)(77)

: 《 》

: 18

: 611731

: 028-87898263

: dfdqpl@dongfang.com

: http://dfdqpl.xml-journal.net/

:

:

:

782

2

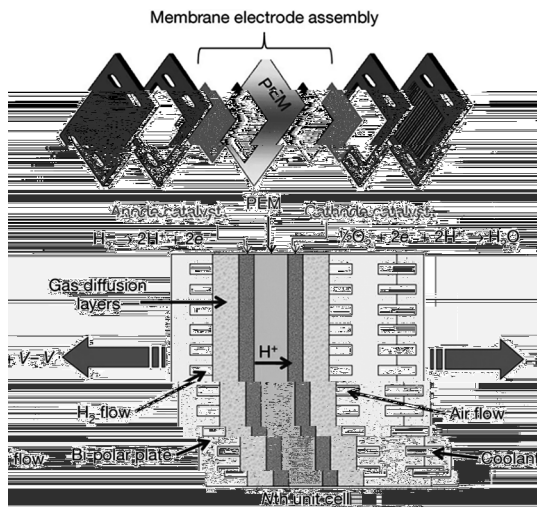


1

1.1

PEMFC

300



1

1.2

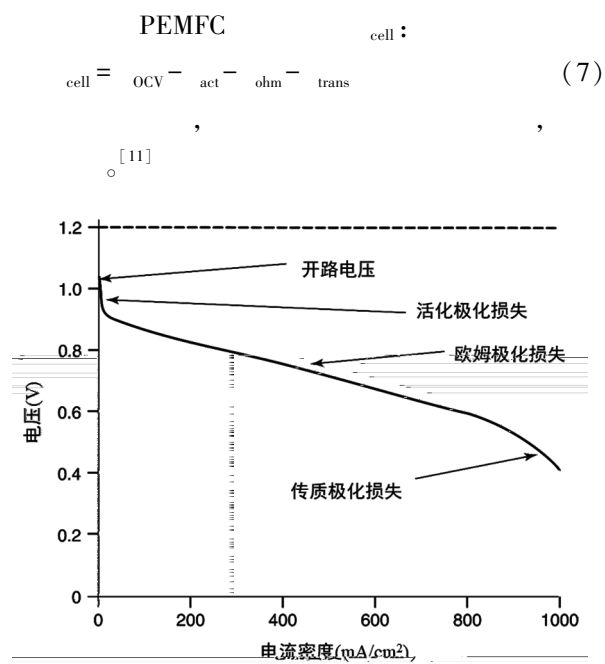


$$\Delta = \frac{\Delta}{\Delta} \quad (4)$$

$$\Delta = \Delta + \Delta \quad (5)$$

$$\Delta_{\max} = \frac{\Delta}{\Delta} \quad (6)$$

PEMFC ( ~1 V ) ( ~1.2 V ) ,



2 PEMFC [11]

2

, PEMFC

, PEMFC

, PEMFC

[13]

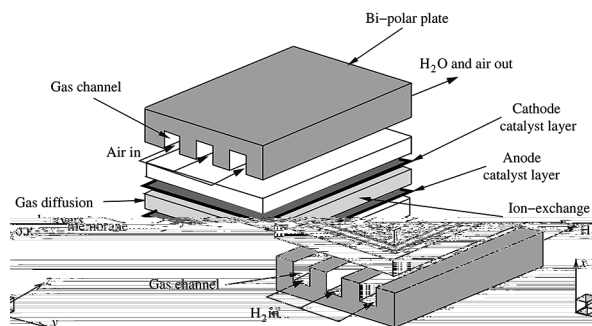
0D、1D、2D

3D

0D

( , , , , , )

1D  
2D  
3D



3 PEMFC [13]

ANSYS

Fluent、COMSOL、STAR-CCM

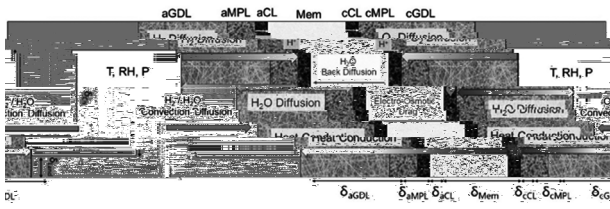
[14]

PEMFC

, Rahman [15]

PEMFC

4) Jiang [16]



4 PEMFC

[15]

PEMFC

[17-18]

PEMFC, Yin [19-20]

PEMFC (5),

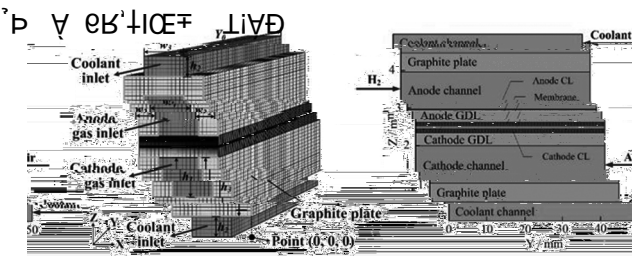
Shimpalee [21]

300 cm<sup>2</sup> PEMFC

Zhang

[22]

PEMFC, 109.93 cm<sup>2</sup>,

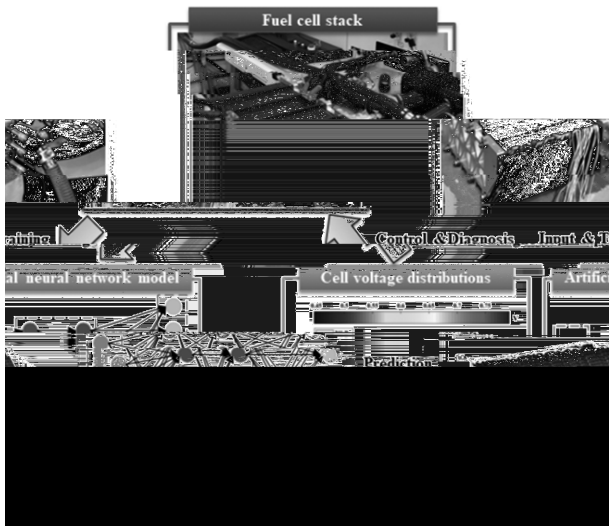


(a)

，  
。ANN  
，  
。Zou [27]  
(ANN)  
(GA) ， PEMFC  
，  
。Tian [28]  
、  
。Su [29]  
，  
60 kW 140  
2 mV,  
( 7)。

( Long Short Term  
Memory, LSTM )  
PEMFC  
LSTM  
，  
。Ma [32]  
(G-LSTM) ， LSTM  
LSTM ，  
。Zhai [33]  
( Advantage

Ac



7

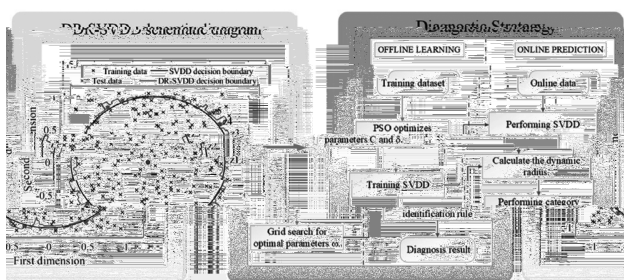
[29]

### 3.2

。Li [30]  
，  
。Liu [31]

Wang [36]

98.5 %。



9

[35]

4

(1)

(2)

(3)

[1] Wang Y, Seo B, Wang B, et al. Fundamentals, materials, and machine learning of polymer electrolyte membrane fuel cell technology [J]. Energy and AI, 2020, 1:100014

[2] [J]. , 2021, 45(12):1660-1664

[3] Pourrahmani H, Yavarinasab A, Siavashi M, et al. Progress in the proton exchange membrane fuel cells (PEMFCs) water/thermal management: From theory to the current challenges and real-time fault diagnosis methods [J]. Energy Reviews, 2022, 1(1):100002

[4] Zhao J, Li X, Shum C, et al. A review of physics-based and data-driven models for real-time control of polymer electrolyte membrane fuel cells [J]. Energy and AI, 2021, 6:100114

[5] Ding R, Zhang S, Chen Y, et al. Application of machine learning in optimizing proton exchange membrane fuel cells: a review [J]. Energy and AI, 2022, 9:100170

[6] [J]. ( ), 2022, 52(9): 2107-2118

[7] George S, Sehgal N, Rana K, et al. A comprehensive review on modelling and maximum power point tracking of PEMFC [J]. Cleaner Energy Systems, 2022, 3:100031

[8] Cai F, Cai S, Tu Z. Proton exchange membrane fuel cell (PEMFC) operation in high current density (HCD): Problem, progress and perspective [J]. Energy Conversion and Management, 2024, 307:118348

[9] Wu D, Peng C, Yin C, et al. Review of system integration and control of proton exchange membrane fuel cells [J]. Electrochemical Energy Reviews, 2020, 3:466-505

[10] Jiao K, Li X. Water transport in polymer electrolyte membrane fuel cells [J]. Progress in energy and combustion Science, 2011, 37(3):221-291

[11] Priya K, Sathishkumar K, Rajasekar N. A comprehensive review on parameter estimation techniques for Proton Exchange Membrane fuel cell modelling [J]. Renewable and Susta

- membrane fuel cells [J]. *Renewable and Sustainable Energy Reviews*, 2019, 113:109283
- [15] Rahman M A, Mojica F, Sarker M, et al. Development of 1-D multiphysics PEMFC model with dry limiting current experimental validation [J]. *Electrochimica Acta*, 2019, 320:134601
- [16] Jiang Y, Yang Z, Jiao K, et al. Sensitivity analysis of uncertain parameters based on an improved proton exchange membrane fuel cell analytical model [J]. *Energy conversion and management*, 2018, 164:639-654
- [17] Xing L, Liu X, Alaje T, et al. A two-phase flow and non-isothermal agglomerate model for a proton exchange membrane (PEM) fuel cell [J]. *Energy*, 2014, 73:618-634
- [18] Xing L, Das PK, Song X, et al. Numerical analysis of the optimum membrane/ionomer water content of PEMFCs: The interaction of Nafion® ionomer content and cathode relative humidity [J]. *Applied Energy*, 2015, 138:242-257
- [19] Yin C, Gao J, Wen X, et al. In situ investigation of proton exchange membrane fuel cell performance with novel segmented cell design and a two-phase flow model

"

# TOPCon

\*

611731

:TOPCon  
。TOPCon  
TOPCon  
TM914 :A :1001-9006(2025)02-0008-04

## The Preparation of Monodisperse Silver Powder Used on the Front Side of TOPCon Solar Cell

\*

(DEC Academy of Science and Technology Co., Ltd., 611731, Chengdu, China)

Abstract: TOPCon solar cells have become the dominant technology of photovoltaic cells because of their high cell efficiency. As the electrode of TOPCon solar cells, silver powder on the front side directly affects the efficiency, so it is the key basic material of the cell. The front side of TOPCon cells requires submicron-sized and monodisperse silver powder with high consistency. Traditionally, monodisperse silver powder has been prepared in two steps: firstly, the silver crystal seed has been prepared, then submicron-sized silver powder has been reduced, but the stability of seed batch production is difficult to guarantee. In this paper, using the template method as a reference, a commercially stable emulsion product is used as crystal seed to replace silver crystal seed produced by a complicated preparation process. At the same time, using emulsion as a template, submicron-sized silver powder is reduced and grown at the interface of emulsion and solution to improve the batch stability of submicron-sized silver powder products and simplify the step-by-step reduction process. In this paper, the feasibility of preparing monodisperse silver powder by using emulsion product as crystal seed and the effect of emulsion product as crystal seed on submicron-sized silver powder were investigated. The results show that the commercial emulsion can be used as crystal seed to prepare highly dispersed and submicron-sized spherical silver powder. As the emulsion product playing a similar role to silver crystal seed, the particle size of silver powder decreasing with the increase of emulsion content shows that the submicron-sized particle size of silver powder can be adjusted by

:2024-09-19

:N (TOPCon/HJT) ; :2F-SC0022094。

: (1983—), ,2010

(1983—), ,2011

:3007734@dongfang.com。



2

2.1

3, 60%,

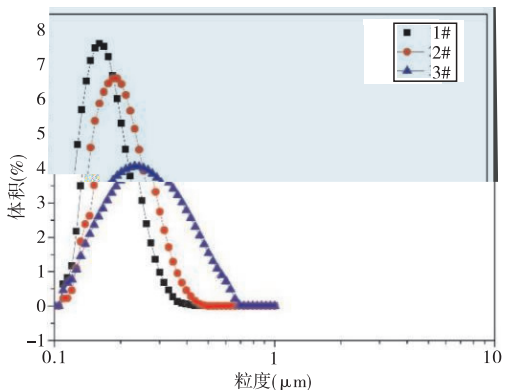
1#、2#、3#。

1 1 :

1 3

$\mu\text{m}$

	D10	D50	D90	D95
1#	0.132	0.178	0.248	0.273
2#	0.147	0.203	0.291	0.321
3#	0.147	0.253	0.446	0.507

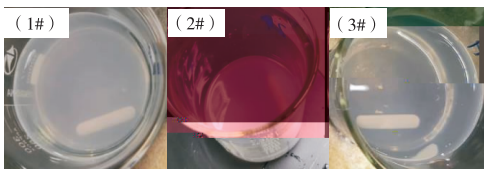


1 3

1、1, 1#、2#、3#

3

2 :



2

1#、2#、3#

2, 3

, 3

, 3

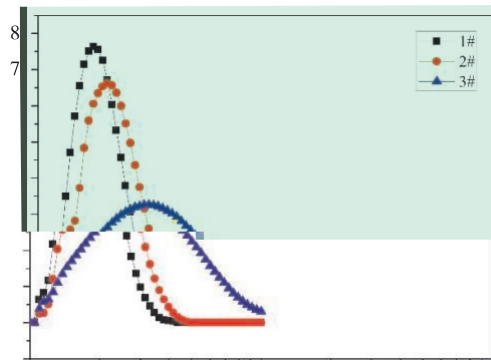
2.2

1#、2#、3#

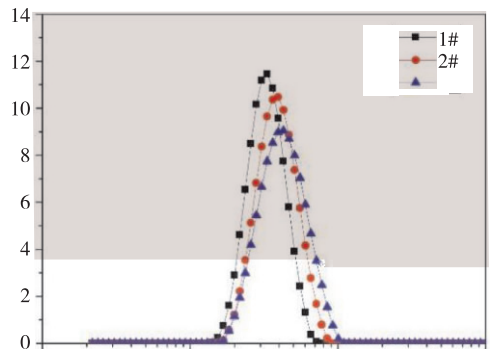
PVP

$V_c$ ,

4



3 3



4 3

2 3

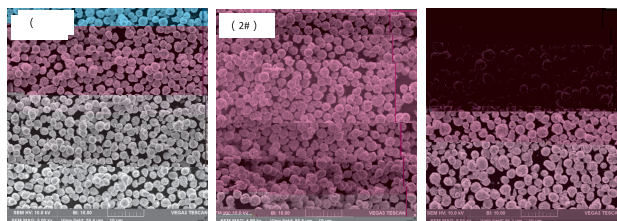
$\mu\text{m}$

	D10	D50	D90	D95
1#	2.168	3.134	4.532	4.986
2#	2.465	3.679	5.505	6.107
3#	2.533	4.007	6.37	7.143

2、4, 1#、2#、3#

3

5

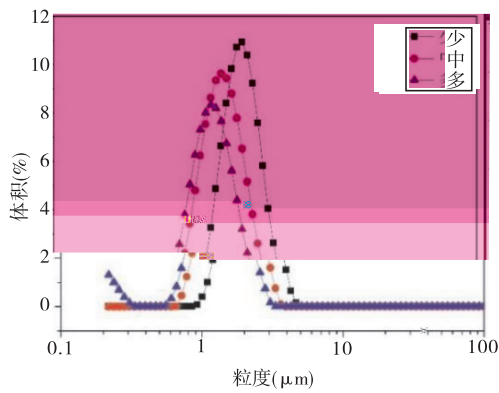
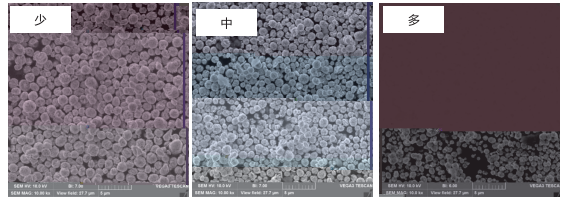


5 (1#)、(2#)、(3#)

5, 3, 1#, 1#

Ag<sup>+</sup> ( [10] ), Ag<sup>+</sup>, Vc, 7(2#)

2.3 1# PVP, Vc, 6 3 :



1#	D10	D50	D90	D95
	1.385	2.039	3.001	3.319
	0.975	1.498	2.316	2.58
	0.18	1.18	1.902	2.14

6, 3, 1#, D50 2.039 μm, 1.18 μm, D10, TOPCon, 1#, 7, TOPCon

7 1# 0



( 10 270 mm× 6 440 mm× 7 315 mm ),  
383 ,

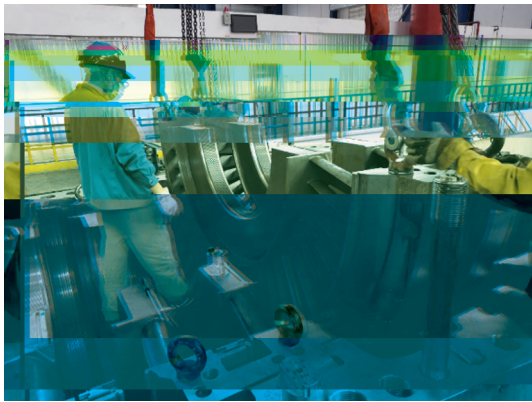
2

2.1

( 2 H ), 3



2



3

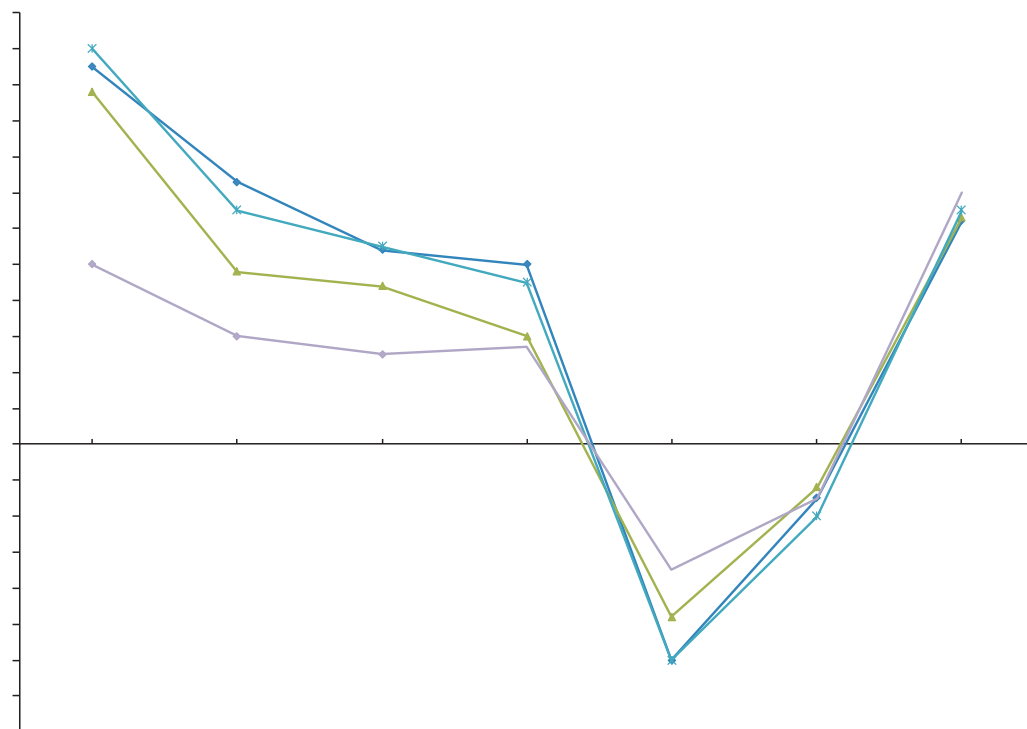
2.2

1

mm

		A1	A2	A3	D1
1	H6	1.05	0.98	1.1	0.5
2	H5	0.73	0.48	0.65	0.3
3	H3	0.54	0.44	0.55	0.25
4	H1	0.5	0.3	0.45	0.27
5	H0	-0.6	-0.48	-0.6	-0.35
6	H7	-0.15	-0.12	-0.2	0.15
7	H9	0.62	0.63	0.65	0.7

4



4

1 4 , 2 :

(1) , H0

(2) D1 H0

: D1 5~8 ,U1 ,U2

3

5、6 7



6



7



8

3.1

、  
 、  
 。  
 1 D1  
 2 9。

mm

		1:	2:	3:	4:	5:
1	H6	0.776	0.32	1.267	-0.001	0.475
2	H5	0.486	0.29	0.703	-0.008	0.275
3	H3	0.446	0.225	0.633	-0.023	0.225
4	H1	0.405	0.185	0.558	-0.008	0.25
5	H0	-0.405	-0.15	-0.562	0.019	-0.285
6	H7	-0.179	0	-0.193	-0.002	0.15
7	H9	0.529	0.15	0.989	-0.004	0.7



9  
2 9 , 2 : , 1,3  
(1) 4, 2,5, 、 ,  
, 2,5 1,3 , : , 。  
:  
, 3.2  
, , ,  
, 、 , ,  
(2) 4 : , 3 10。  
3 mm

		1:	2:	3:	4:
1	H6	0.119	0	0.525	—
2	H5	0.18	0.045	0.833	0.8
3	H3	0.262	0	1.19	1.075
4	H1	0.355	0.025	1.526	1.35
5	H0	0.402	0.025	1.674	1.45
6	H7	0.405	0.055	1.55	1.5
7	H9	0.236	0.05	0.849	—



10

3 10

:

。

,

。

:

4

[1] , , .

[J]. ,2022(4):36-41

[2] . : :

[M]. : ,1999

[3] . [J].

,2014(1):1-6+12

[4] , . [J].

,2014(2):5-10



,

!

:TM623

:A

:1001-9006(2025)02-0018-04

## Design Optimization of High Pressure Outer Cylinder of the GEN-IV Nuclear Power Ultra-high Pressure Steam Turbine

(Dongfang Turbine, Co., Ltd., 618000, Deyang, Sichuan, China)

Abstract: With the progress and development of nuclear power technology, the GEN-IV nuclear power plant has gradually begun to be commercialized, and its main steam parameters can reach the level of conventional thermal power ultra-high pressure steam turbines, but the characteristics of the high-pressure outer cylinder are very different from those of thermal power units and PWR nuclear power u

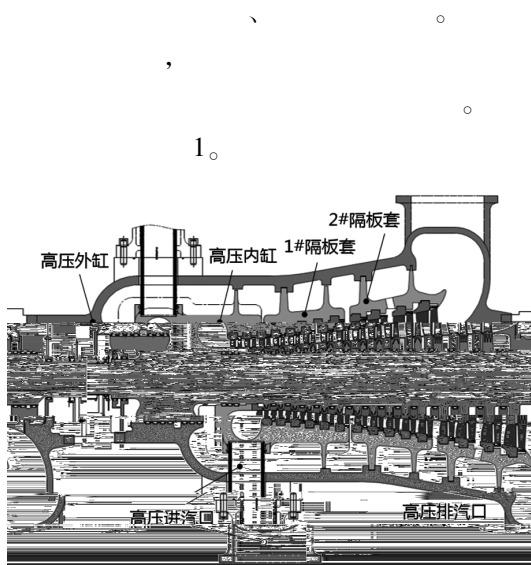
收 稿 日 期

年

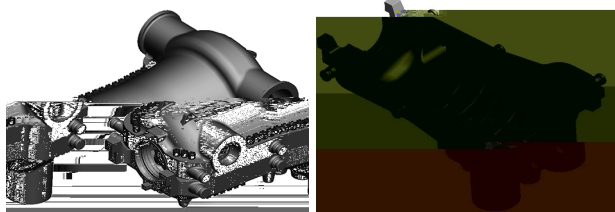
月

:2024-08-14

: (1984—), ,2005



1

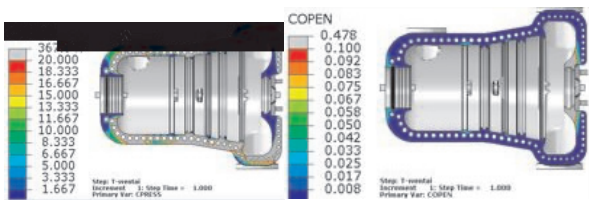


2

## 2

### 2.1

(3) : , 20 MPa( 5) ,



5 : : MPa, : mm

3

3.1

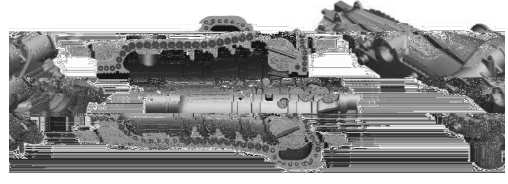
[6] ,

3.1.1

(1) , ; (2) ,

3.1.2

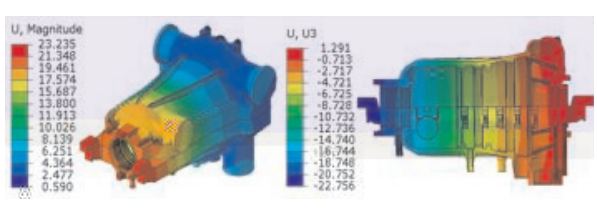
(1) , (2) ,



6

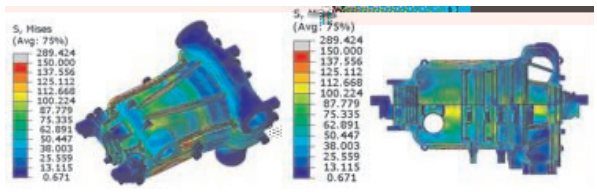
3.2

(1) : , ( 7) ,



7 (mm)

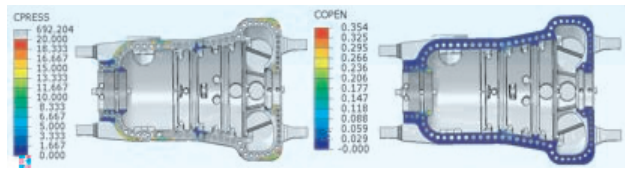
(2) : 100 MPa , 185 MPa , 245 MPa( 8) ,



8 (MPa)

(3) : , 20 MPa

( 9) , 1#

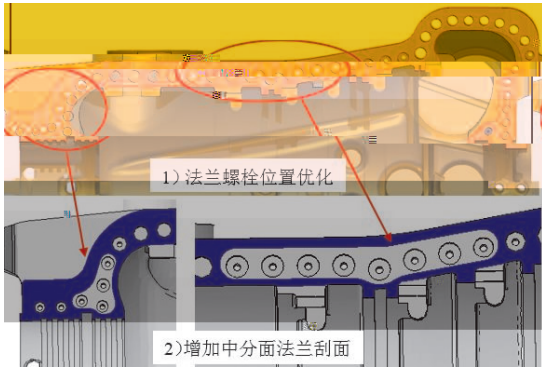


9 : : MPa, : mm

3.3

1# , [7] ,

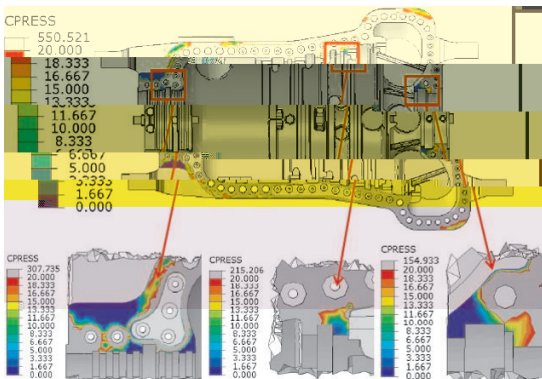
10



10

11

0.01 mm



11

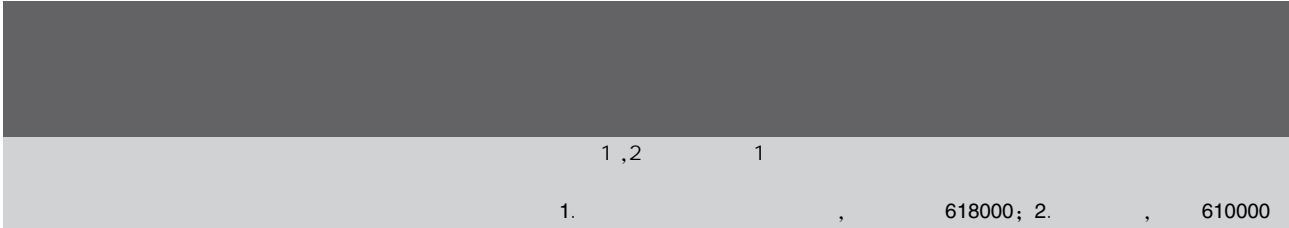
(MPa)

4

- [1] [J]. ,2013, 27(3):36-43
- [2] [M]. : ,1999
- [3] , .300 MW [J]. ,2007(2):27-32
- [4] [J]. ,2023(3):10-15
- [5] , .1 000 MW [J]. ,2016,31(10):32-37+124
- [6] [J]. ,2020(2):15-18
- [7] [J]. ,2020(2):75-78

,

!



1,2 1  
1. , 618000; 2. , 610000  
:  
,  
,  
,  
:  
; ;  
:TP273;TM614 :A :1001-9006(2025)02-0022-06

## Damping Control of Flexible Tower Side-side for Wind Turbine

1 2 1

(1. Dongfang Electric Wind Power Co., Ltd., 618000, Deyang, Sichuan, China;

2. Sichuan University, 610000, Chengdu, China)

Abstract: Taking the flexible tower of a large wind turbine as the research object, first analyze the tower structure dynamics and aerodynamic model, and combine the system dynamics model to study the feasibility of torque control on the right and left vibration damping control of the tower, through linearization the controllability rank criterion of the model is proved. Based on the measured values of the left and right accelerations of the tower top, the left and right vibration speeds of the tower top are obtained through the integration link to design a tower left and right damping controller. Finally, simulation and field tests verify the effectiveness of the algorithm, which can reduce the vibration value of the tower on the left and right, which is of great significance to ensure the safe operation of the wind turbine.

Key words: wind turbine; flexible tower; tower side-side vibration; damp controller

, , ,  
○  
, 、  
,  
, ,  
, , ,  
,

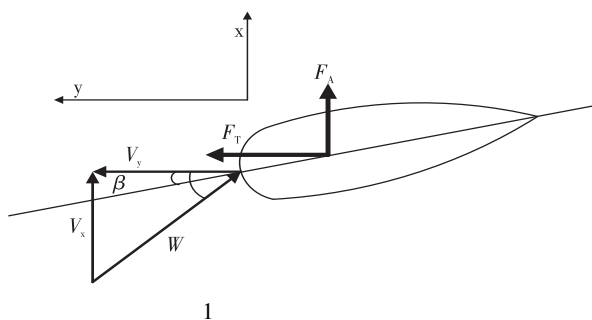
:2024-07-16

: ; :2022YFB4201303。

: (1985—), , ○

[9]

[10]



$$x = \infty(1 - ) + x \quad (7)$$

$$y = (1 + ) + y \quad (8)$$

1

1.1

(1)

(2)

$$( ) ( ) + ( ) ( ) + ( ) ( ) = \quad (3)$$

$$A - G = \quad (4)$$

1.2

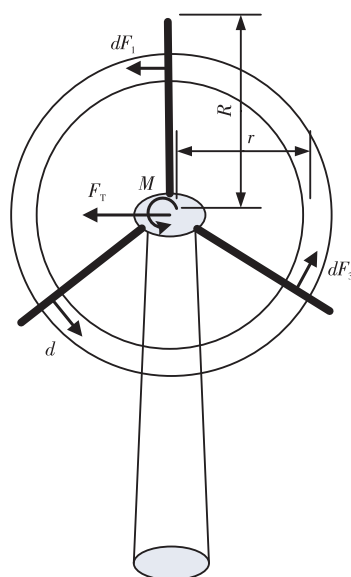
$$A = ( x, y, ) \quad (5)$$

$$T = ( x, y, ) \quad (6)$$

(BEM)

[11]

$$A = T \times \quad (9)$$



$$A = \int_1^2 A \quad (10)$$

$$T = \int_1^2 \cos T \quad (11)$$

$$A = \int_1^2 A \quad (12)$$

1.3



$$= \begin{bmatrix} 0 & 1 & 0 \\ -\frac{p}{p} & \frac{\partial}{\partial} & \frac{\partial}{\partial} \\ 0 & \frac{\partial}{\partial} & \frac{\partial}{\partial} \end{bmatrix},$$

$$= \begin{bmatrix} 0 & 0 & 0 \\ \frac{\partial}{\partial} & \frac{\partial}{\partial} & 0 \\ \frac{\partial}{\partial} & \frac{\partial}{\partial} & -1 \end{bmatrix} \quad (32)$$

$$= [0 \ 1 \ 0],$$

$$\text{rank}[\dots] = 3$$

$$= \begin{bmatrix} 0 & 0 & -1 \end{bmatrix},$$

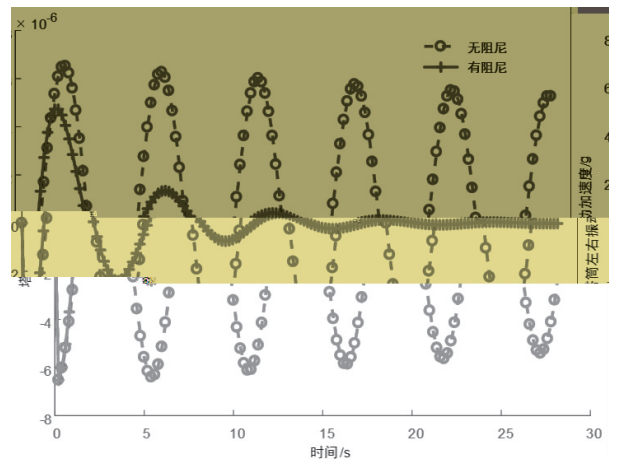


(34)

$$() = - \times \frac{2}{2} \frac{2}{2} \frac{1}{1} + 1 \times \frac{1}{2} \frac{2}{2} \frac{3}{3} + 1 \quad (34)$$

		Nm/(m/s)	57 245
1	1	rad/s	7.5
1	1	-	0.1
2	2	rad/s	4.6
2	2	-	0.5
	3	rad/s	6.5
	3	-	1

Simulink

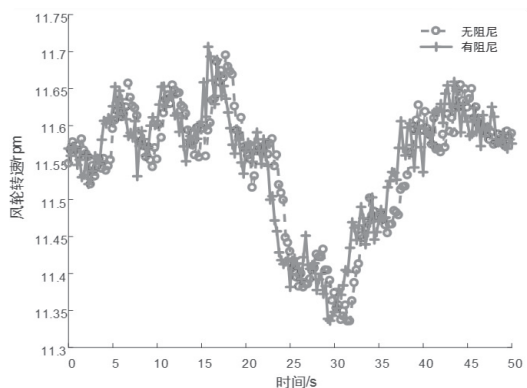


4

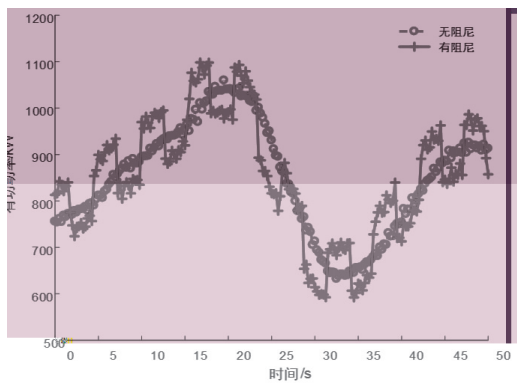
2.3 Bladed [12],

(m)	127
(m)	120
(Hz)	0.18
(r/min)	13.3
(kW)	2 000

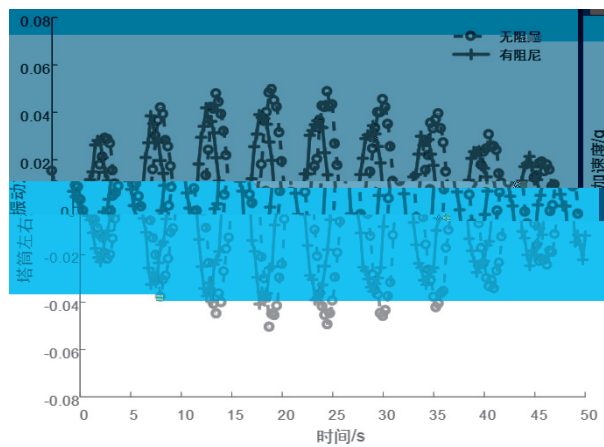
0.177 Hz,  
3  
11.55 r/min  
1P 0.192 Hz,  
7%。



5



6

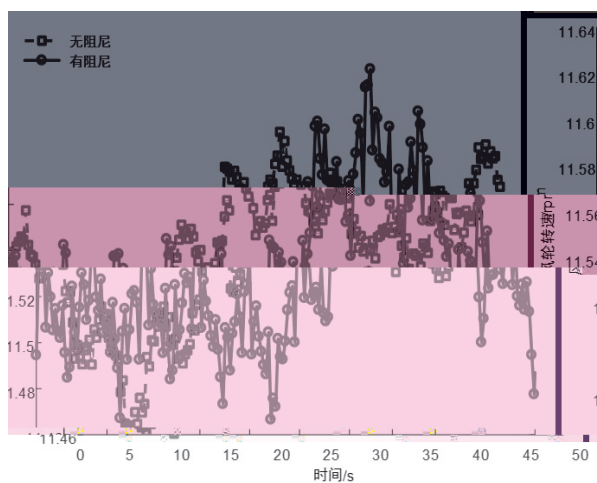


7

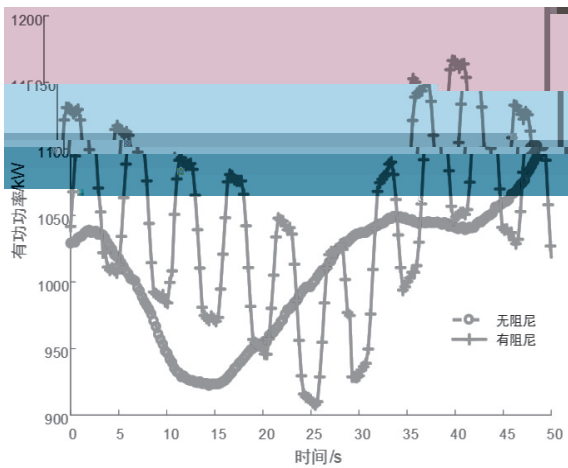
5~7  
20 s~40 s  
11.35 r/min, 1P  
5%。

3

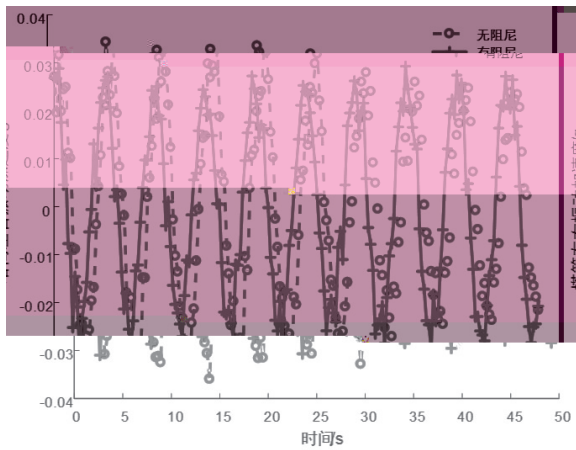
8~10



8



9



10

3、4:

3

(g)	0.049	0.042	16.67 %
(g)	0.034	0.029	17.24 %

4

(g)	0.036	0.029	24.14 %
(g)	0.023	0.020	15.00 %

3、4

4

，  
○  
，  
，  
○

：

[1] ， ， ， .  
[J]. ，2016,36(1) :75-83

[2] ， ， ， .  
[J]. ，2020,42(S2) :248-253

[3] ， ， ， . TMD  
[J]. ，2020,41(10) : 276-284

[4] ， ， ， .  
[J]. ，2022(19) :81-83+88

[5] . [D].  
，2017

[6] ， ， ， .  
[J]. ，2023,44(10) :  
296-304

[7] ， ， ， . [J].  
，2014,31(3) :325-329

[8] ， ， ， ， .  
[J]. ，2015,36(1) :54-60

[9] ， ， ， ， . LESO  
[J]. ，2018,38(19) : 5854-5862  
+5943

[10] ， ， ， ， .  
[J]. ，2020(4) :80-83

[11] Tony Burton, Nick Jenkins, David Sharpe, et al. Wind Energy Handbook, 2nd Edition[M]. Wiley, 2011

[12] Bossanyi E. A. GH bladed user manual [R]. Bristol: Garrand Hassan and Partners Limited, 2009.



，  
！

618000

2 MW

:TM315

:A

:1001-9006(2025)02-0028-05

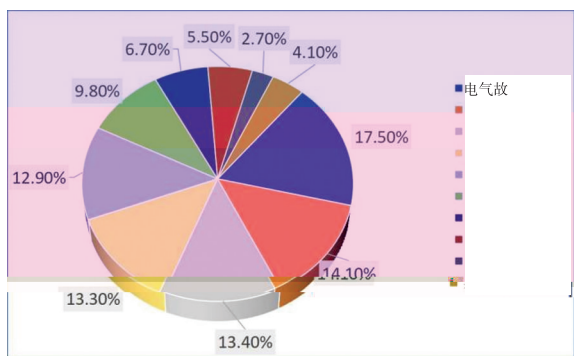
## Analysis of Shaft Deformation in Abnormal Working Conditions of the PMSG

Electric Machinery Co., Ltd., 618000, Deyang, Sichuan, China)

Abstract: As the core of a wind turbine, the motor is very important for long-term safety and stability. When a 2 MW permanent magnet synchronous generator (PMSG) in an extreme weather of typhoon was coming, the brake failed, and the brake disc could not be released, resulting in sharp wear of the brake disc. The brake disc was located in the motor shafting.

:2024-08-09

: (1994—), ,2016



1

1

1.1

2 MW

2 11

1.2

2023 10

2

(1)

(2)

(3)

(4)

( )

0.25 ~ 0.68 mm,

0.16 mm;

1

mm

	1	2	3	4	5	6	
	-0.28	-0.2	-0.12	-0.14	-0.21	-0.27	-0.203
D+	-0.06	+0.02	+0.09	+0.06	-0.01	-0.05	+0.008
0.48	+0.18	+0.25	+0.27	+0.25	+0.24	+0.21	+0.233
H+	+0.16	+0.17	+0.17	+0.16	+0.16	+0.17	+0.165
0.01							

(5)

33 mm( 40 mm),

(6)

3

QT400

0.6~0.8 mm。

### 3.1

2:

2

	MPa		kg/m <sup>3</sup>	MPa	MPa
QT400	$1.69 \times 10^5$	0.275	$7.1 \times 10^{-9}$	220	360
QT400	$1.69 \times 10^5$	0.275	$7.1 \times 10^{-9}$	220	360
Q345D	$2.10 \times 10^5$	0.3	$7.85 \times 10^{-9}$	285	450

### 3.2

### 3.3

#### 3.3.1

mm

3 :

3

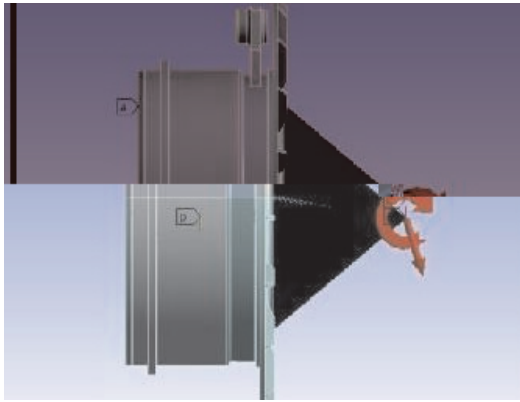
/						
mm	kg	kg/m <sup>3</sup>	MPa	-	N	Nmm

#### 3.3.2

2 MW

2

GL  
GL  
L。 5



5

3.5

0~  
2.6 r/min。  
8~30 m/s,  
 $M_x, M_y, M_z, F_x, F_y, F_z$   
[3]

4 :

4

$M_x$	$M_y$	$M_z$	$F_x$	$F_y$	$F_z$	
kNm	kNm	kNm	kN	kN	kN	-
960	-7 500	-600	-260	45	-850	1.5

3.6

[4]  
600 °C,  
340 °C。 6



6

#



# PLM

1,2

1.

, 611731; 2.

, 611731

NET ; PLM; ; TK222 ; A ; 1001-9006(2025)02-0033-05

## Development of Calculation Software for Boiler Pipe Insulation Materials Based on PLM

1 2

(1. Dongfang Boiler Co., Ltd., 611731, Chengdu, China;

2. Clean Combustion and Flue Gas Purification Key Laboratory of Sichuan Province, 611731, Chengdu, China)

Abstract: In the field of boiler pipeline design, insulation design is a critical link to ensure heat transfer control of pipe walls and stability of steam parameters. Faced with diverse temperature and diameter specifications of boiler connecting pipes, as well as the diversity of insulation material layers and quantities, accurate and efficient calculation of insulation material quantity is crucial for enterprises. This study employs the VB. NET programming language to develop dedicated design software. The software significantly improves the efficiency and quality of insulation design work through innovative automated design. The proposed technical solutions and development strategies not only provide practical tools for boiler pipeline insulation design but also offer reference value for similar developments.

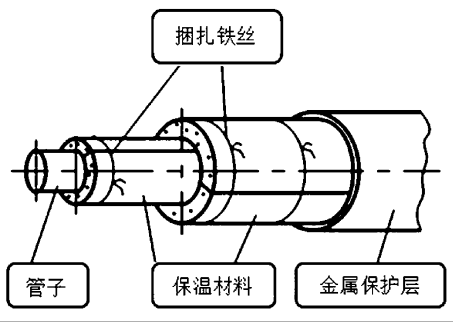
Key words: PLM; insulation material; calculation software; software development

:2024-09-20

: (1980—), ,2004

:mailguofeng@163.com。

(3) : 1 m Excel , , 。  
 , , 1 m PLM 。



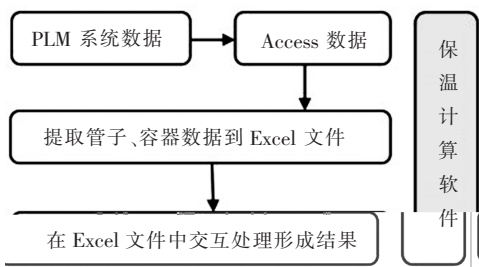
1

Excel

3

PLM( ) ,

2



2

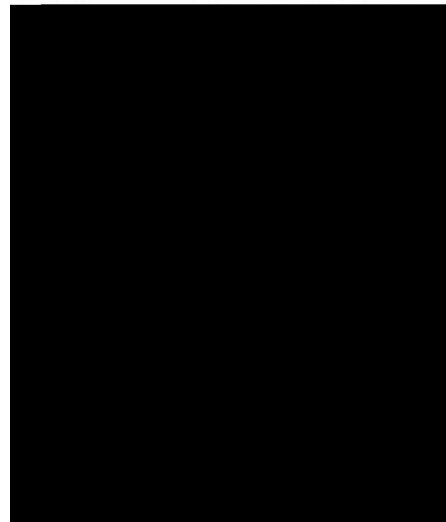
1

### 1.1 PLM

, ,

Excel , , 。 PLM 。  
 、 、 “ ” ,  
 “φ × ; L = ( )”。

PLM ,  
 mdb Access  
 , 3。



3

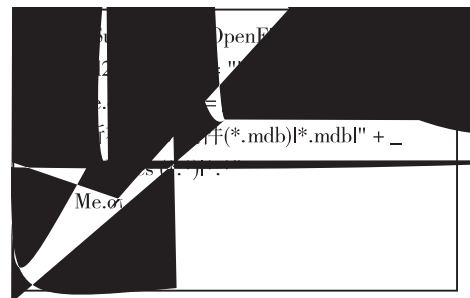
Access

### 1.2 VB.NET

VB.NET( Visual Basic. NET)

#### 1.2.1

VB.NET ( 4), [1]  
Access , 、



4

Access

1.2.2

(Regular Expression)

(Pattern),

[2-3], “φ ×”,  
“[Φ|φ](\d+\.\ \* \d\*) [×|x|X](\d+\.\ \* \d\*)”,  
: “Φ” “φ”,  
( ), “×( )”、“x”( ) “X”( ),  
( 1, )。

1

φ mm×δ mm	kg	mm	mm	mm
φ28×4	20G	118	28	4 49 841.5
φ159×16	20G	134	159	16 2 374.8
φ159×16	20G	274	159	16 4 856
φ273×28	20G	926	273	28 5 473.6
φ273×28	20G	1110	273	28 6 561.2

1.2.3 Excel

VB.  
NET COM, Excel  
[4-5] Excel

1.3

,  
Excel

1.4

Excel

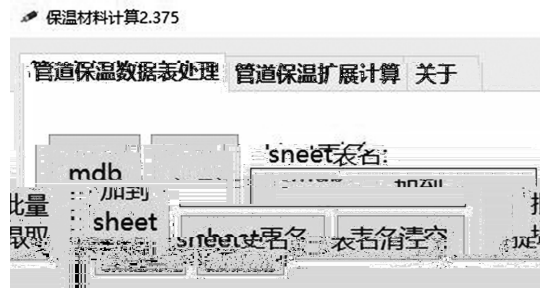
2

, “ → → → ”  
2019 3 2023 11 ,  
70 ,  
“Φ” “φ”,  
( ), “×( )”、“x”( ) “X”( ),  
( 1, )。

3

3.1

“ ” “  
” ( 5)。  
3.1.1  
“ ”  
(1) Access  
( 5 , “mdb” )  
, Excel ( “sheet” )。 mdb  
( 5 “sheet” )。



5 ( )  
(2) Excel , mdb  
“ ”,  
、



6

1 100 mm

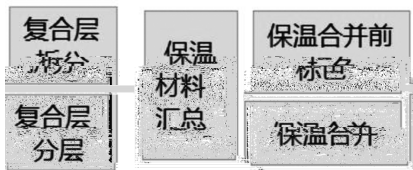
“ ” ，  
Excel

( 2, 1 940 mm, 1 780 mm, 80 mm )。

2 ( )

mm	mm	℃	mm
1 780	7 000	500	80
1 940	7 000	500	120

(3) ” 7 “



7

( )

30 mm)

### 3.1.2

(1)

1 100 mm

(2)

φ38

( 8)。



8

(3)

( 9)。

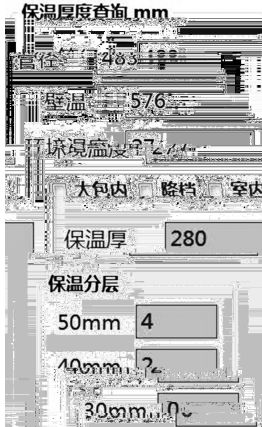
h



9

(4)

(10)。



10

### 3.2

(1) Excel

(2)

(3)

(4)

(5)

(6)

PLM

(7)

### 3.3

3

	S/N/M	K/H/J/A/B
	15	12.5
	10	7.5
	5	3
	4	3
	200 %	317 %
	150 %	150 %

4

[1]

[2]

[3]

[4]

# 300 Mvar

618000

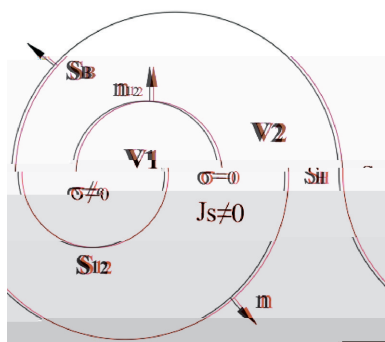
: , 300 Mvar  
。 300 Mvar  
412 MVA 。 0 !

:2024-09-14

: (1984—), , ,

。 :xiaojian2005e@126.com。





3

$$\left. \begin{aligned} \nabla \times (\nabla \times \mathbf{A}) - \nabla (\nabla \cdot \mathbf{A}) + \frac{\partial}{\partial t} \nabla \phi &= \mathbf{J} \\ \nabla \cdot \left( -\frac{\partial}{\partial t} \mathbf{A} - \nabla \phi \right) &= 0 \end{aligned} \right\} \quad (1)$$

$$\nabla \times (\nabla \times \mathbf{A}) - \nabla (\nabla \cdot \mathbf{A}) = \mathbf{J}_s \quad (2)$$

$$\left. \begin{aligned} \nabla \times \mathbf{B} &= \mathbf{J} \\ \nabla \cdot \mathbf{B} &= 0 \end{aligned} \right\} \quad (3)$$

$$\left. \begin{aligned} \nabla \cdot \mathbf{H} &= \mathbf{J}_s \\ (\nabla \times \mathbf{H}) \times \mathbf{m} &= 0 \end{aligned} \right\} \quad (4)$$

$$\left. \begin{aligned} \mathbf{A}_1 &= \mathbf{A}_2 \\ \nabla \cdot \mathbf{A}_1 &= \nabla \cdot \mathbf{A}_2 \\ (\nabla \times \mathbf{A}_1) \times \mathbf{m}_{12} &= \\ (\nabla \times \mathbf{A}_2) \times \mathbf{m}_{12} &= \\ \nabla \cdot \left( -\frac{\partial}{\partial t} \mathbf{A} - \nabla \phi \right) &= 0 \end{aligned} \right\} \quad (5)$$

12, B, H; 12  
12, 1, 2; s

3

3.1 412 MVA

412 MVA 10 %

4~9 4

5, 6

7, 8

, 9

3.2

4

3.80E+07  
3.42E+07  
3.04

5

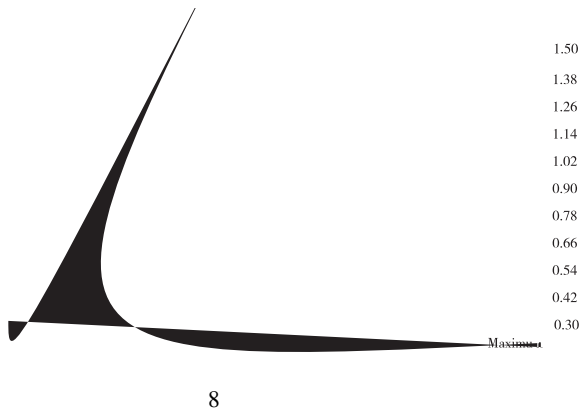
Magnetic Flux Density  
Contour

6

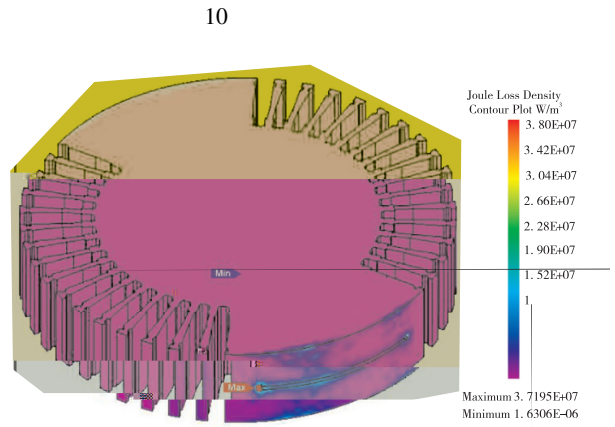
Joule Loss Density

Maximum 3.3585E+06  
Mi

7



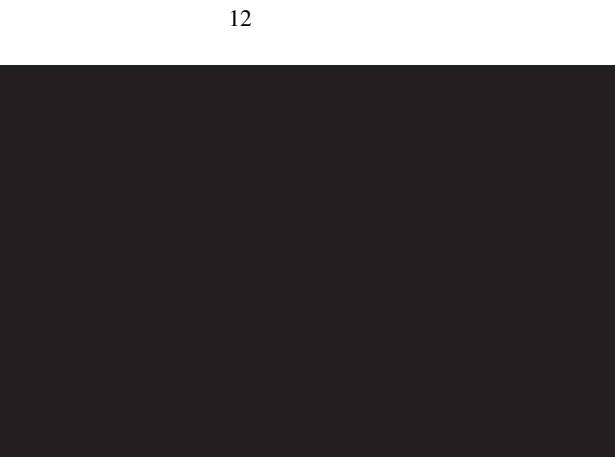
8



10



11



12



13

9

2 412 MVA (kW)

	10 %	15 %
1.45	5.96	11.77
0.85	2.03	3.65
0.92	0.43	0.95
3.22	8.42	16.37

∴

，

，

。

，

。 412 MVA 10 %

， 3.79E7

W/m<sup>3</sup>； 3.36E6 W/m<sup>3</sup>；

1.07E6 W/m<sup>3</sup>。

3.2 300 Mvar

300 Mvar 15 %

10~15 。

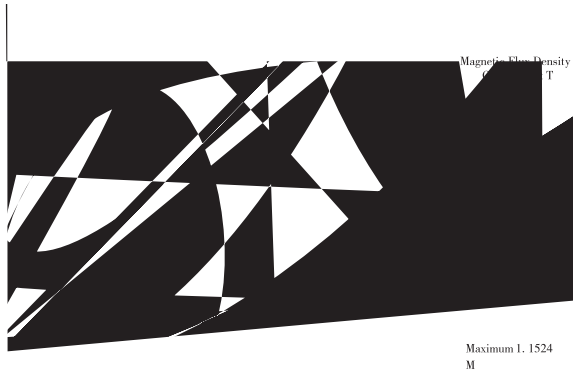
10

， 11 ， 12

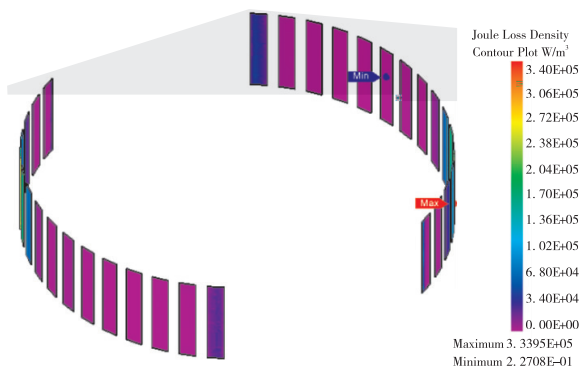
， 13 ， 14

， 15

。



14



15

Mvar , 、 412 MVA 300 (2)

10 % , 412 MVA  
3.79E7 W/m<sup>3</sup>; 300 Mvar (3)

15% , ,  
3.72E7 W/m<sup>3</sup>。 412 MVA  
10.4 % , 412

MVA  
$$= \left(\frac{0.104}{0.1}\right)^2 \times 3.79 = 4.0993 \text{ (E7 W/m}^3\text{)}$$

300 Mvar

o  
$$_2 = \sqrt{\frac{4.0993}{3.7195}} \times 15\% = 15.75\%$$

300 Mvar

15.75 % o

6

412 MVA

300 Mvar

412 MVA

300 Mvar

:

(1) 300 MVar

15.75 % ,

:

[1] D. Ban, D. Zarko and Ivan Mandic. Turbogenerator end-winding leakage inductance calculation using a 3-D analytical approach based on the solution of Neumann Integrals. IEEE Trans. on Energy Conversion, 2005, 20: 98-105

[2] , , . 1000 MW [J]. , 2008, 28(14): 118-121

[3] , , . 330 MW [J]. , 2008(4): 51-54

[4] , , , . 2004, 24(11): 112-113

[5] . [D]. , 2011, 17-19

[6] . [D]. , 2006, 8-11

[7] , , , . 300 MVar [J]. , 2016, 30(3): 19-23

[8] , . 600 MW [J]. , 2004, 18(1): 20-23

:

、 , 《 》 2025 3 25

:

1: <http://dfdqpl.xml-journal.net/> , “ / ”。

2: <https://www.manuscripts.com.cn/dfdqpl>。

manuscripts.com.cn/dfdqpl

dfdqpl@dongfang.com

o

: 028-87898263;

: dfdqpl@dongfang.com

《 》

2025 3 25

# Workbench

618000

: Workbench 333 633  
: ; ; ;  
:TK263 :A :1001-9006(2025)02-0044-06

## Research on Vibration Characteristics of Steam Turbine Low Pressure Blade Based on Workbench

(Dongfang Turbine Co., Ltd., 618000, Deyang, Sichuan, China)

Abstract: The pre-stress modal analysis of low pressure 333 blade and 633 blade is carried out by the workbench. There are two modes of analysis for each blade. One method considered the contact behavior between adjacent shroud. The other is to calculate the resonance frequency by the shroud imprinting surface method. Both modes change the contact mode of shroud and blade root respectively to simulate the real contact stiffness as much as possible. The resonant frequencies of the blades under different calculation modes are obtained, and the resonant frequencies are compared with the experimental results. The calculation method closest to the test results is found. It provides a reference for the vibration design of subsequent blades.

Key words: vibration; finite element; blade; contact

:2024-09-23

: (1986—), ,

,  
o ,  
o ,  
, [3]  
o  
o  
,  
(  
)333 ( )633  
o ,  
,  
, o  
,  
,  
, o  
,  
,  
o  
,  
,  
o  
,  
o

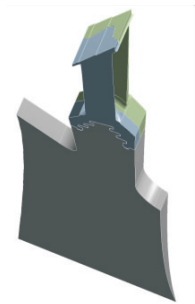
1 333 633

333 1 o 333  
V , ,

1 , 2 3 300 r/min 6 1  
。 1 2 K=6 3  
6 1 ,  
 , 。

3 333

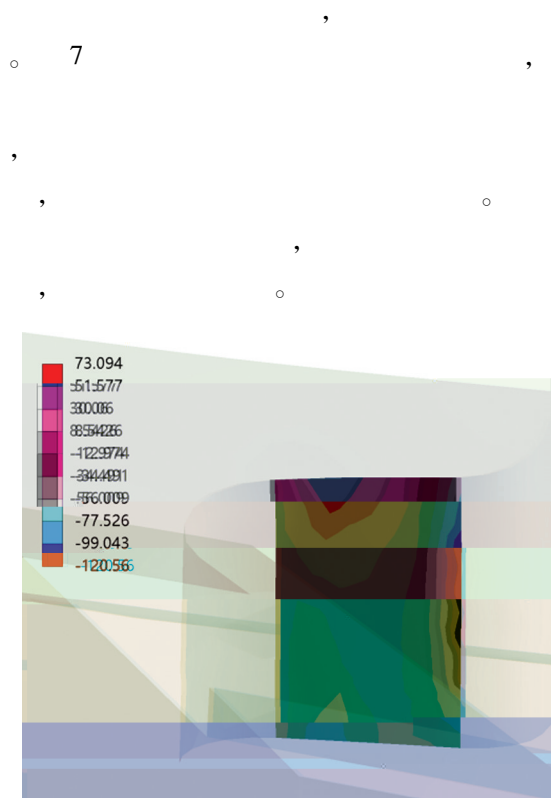
333 3  
。 ,  
。 :  
(1) ;  
(2) ;  
(3) ;  
(4) 3 000 r/min 3 300 r/min  
 ;  
(5) ;  
(6)  
。



5 333  
333 6 1 7  
1 。 333  
1 。 333 6 1

312.2 Hz, 7 1 317.6 Hz。  
。  
、 、 , 5  
。  
6 333 , ,  
6 1 7 1 。。

1  
2 Hz  
-15.8  
MPa。



7 333

8

1

31.2 MPa,

0。

6.8 MPa。

333

9

3

2 333

	/Hz		/Hz	
	6	7	6	7
1	310.48	313.6	-1.72	-4
	294.55	297.28	-17.65	-20.32
2	308.72	311.4	-3.48	-6.2
	292.15	294.48	-20.05	-23.12
3	315.6	320.78	3.4	-13.38
	299.42	304.22	-12.78	3.18

2

,6,7

-6.2~3.4 Hz

6,7

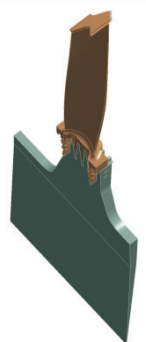
12.8~

23.1 Hz。

4 633

633

11



11 633

(1)

(2)

(3)

(4)

;

(5)

(6)

633

2 633

3 633

325.6 Hz,7

2

312.7 Hz。

4

3 633

	/Hz		/Hz		/MPa
	6	7	6	7	
	357.67	342.84	32.07	30.14	-190.5
	131.58	131.4	-194.02	-181.3	5.6
	139.12	138.08	-186.48	-174.62	5.6
	328.55	315.66	2.95	2.96	-166.6

12

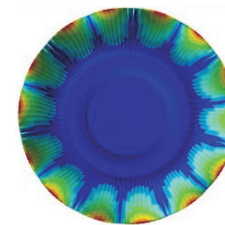
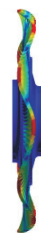
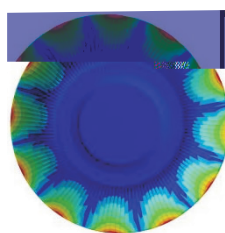
633

6

2

7

2



12 633

6

2

( )

7

2 ( )

3

633

6

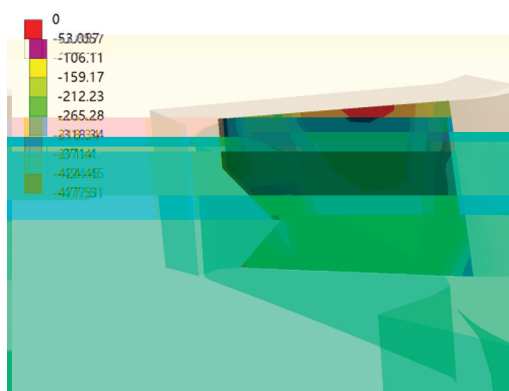
2

7

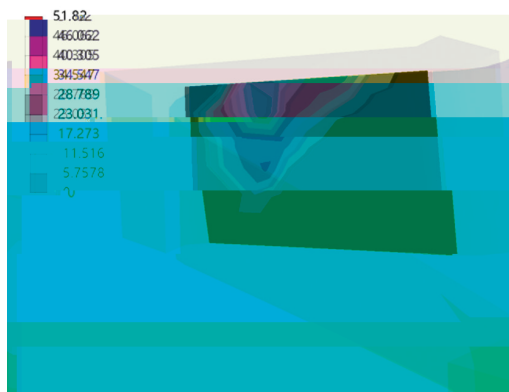
2

2

2.95 Hz,  
633  
3  
2.95 Hz  
-166.6 MPa  
13



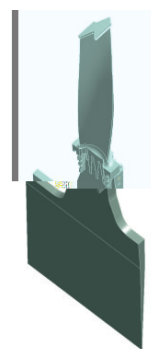
13 633



14 633

14 3  
51.8 MPa,

0  
5.6 MPa  
633  
15  
3  
16  
1  
2  
3



15 633



16 633

633

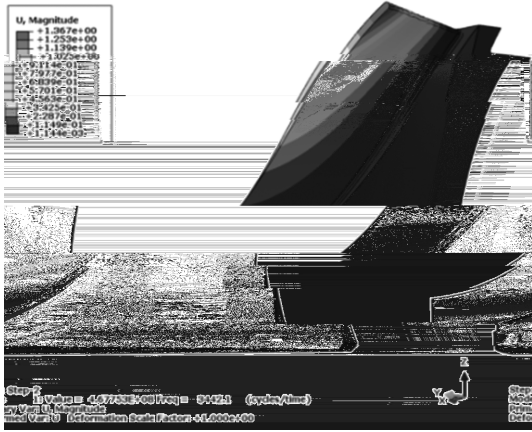
4 633

	/Hz		/Hz	
	6	7	6	7
1	341.78	332.17	16.18	19.47
	317.83	308.75	-7.77	-3.95
2	357.76	342.93	32.16	30.23
	329.61	316.73	4.01	4.03
3	339.06	330.18	13.46	17.48
	315.64	307.08	-9.96	-5.62

( 53 )







4

## 2.2

， ， 。  
，  
，

2

				(Hz)
	2 143	2 057	2 125	2 128
	2 131	2 135	2 134	2 134
	12	78	9	6
	1 421	2 198	3 408	3 947
	3 055	3 528	3 735	4 023
	1 634	1 330	328	76

3

(3)

(1)

(2)

n

610213

5G

:F424;TH16

:A

:1001-9006(2025)02-0054-09

## Intelligent Manufacturing: Leading the Direction of Future Industrial Development

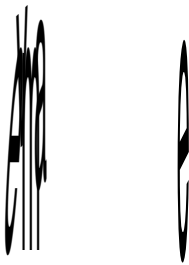
(Tianfu Yongxing laboratory, 610213, Chengdu, China)

Abstract: With the rapid development of global technology, traditional manufacturing is facing challenges such as resource and environmental pressures and changes in market demand, leading to issues such as inefficiency and environmental pollution. Intelligent manufacturing, as a key solution to these problems, integrates information and communication technology with advanced manufacturing technology to digitalize, network, and smarten the manufacturing process. This paper conducts an in-depth discussion on intelligent manufacturing, grasps the trends of future industrial development,

explor

t

n r



:2024-01-09

: (1982—), , ( ), .



[8]

(4) :

[8]

(5) :

[8]

1.4

(1) : (RMS),

(2) :

(3) :

2

2.1 (IoT)

(IoT),

RFID,

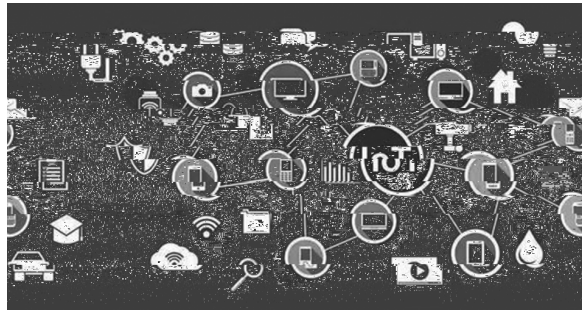
1

[9]

5G

AI

[10]



1

2.2 (AI)

(AI)

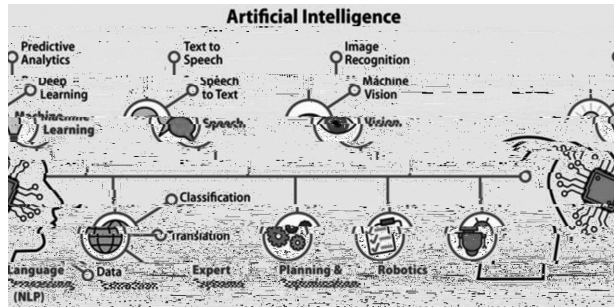
2

AI

[11-12]

AI

[13]



2 AI

2.3

2.5

3

[14-15]

[16]



3

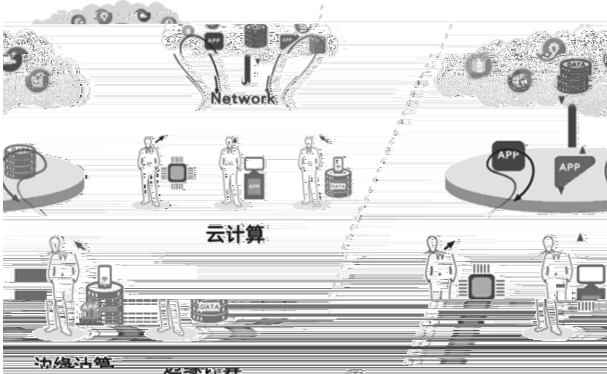
2.4

[17]

4

AI

[18]



4

5

[19]



5

3

3.1

6



9

3.5

( 1 )

(AGV)

5G

(2)

[4]

4

(3)

4.2

(1)

4.1

(1)5G

:5G(

5G

VR

5G

、AR/

、  
(2)  
、  
、  
、  
、

AI : , AI

5.1

ISO/IEC 27001

(1)

(2)

TCM/TPCM)

(2)

( AiDLP ),  
NLP

( HTTP/FTP/SMB )

AiDLP

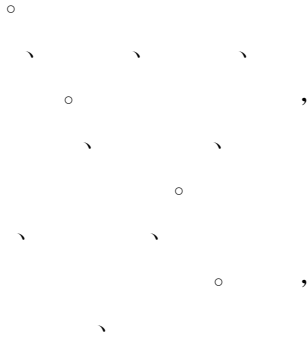
(3)

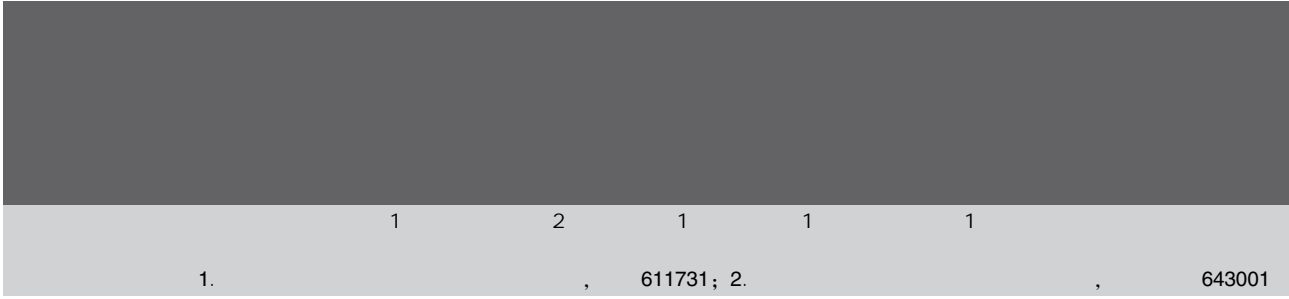
U

5.2

6

(1)





1. , 611731; 2. , 643001

: , , ,

, SICK , ,

, ,

: ; ; ;

:TK226 ;A :1001-9006(2025)02-0063-05

## Research on Weld Bevel Dimension Detection of Boiler Tubes Based on Line Laser Scanning

1 2 1 1 1

(1. DEC Academy of Science and Technology Co., Ltd., 611731, Chengdu, China;  
2. Dongfang Boiler Co., Ltd., 643001, Zigong, Sichuan, China)

Abstract: In the manufacturing process of power plant boilers, the quality of small diameter pipe joint groove processing is the decisive factor that determines the quality of joint welds. After the automation of small diameter pipe material preparation, the consistency of groove processing quality fluctuates greatly due to the influence of tool cha

:2024-08-26

: (1992—), ,2016

, 2D,3D

[3] , 1(a) 。

25 mm~65 mm ,

SICK

1(b) 。

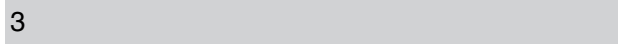


1

，  
，  
[4]

，  
xx mm ,  
xx m/s , 2

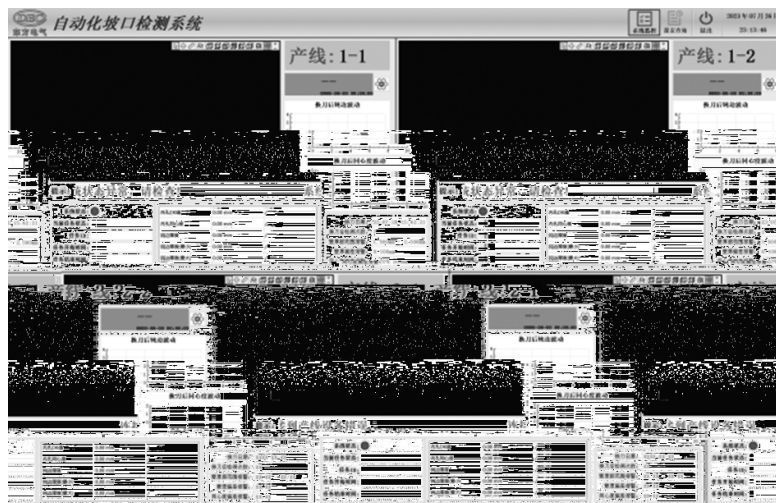
STEP1:



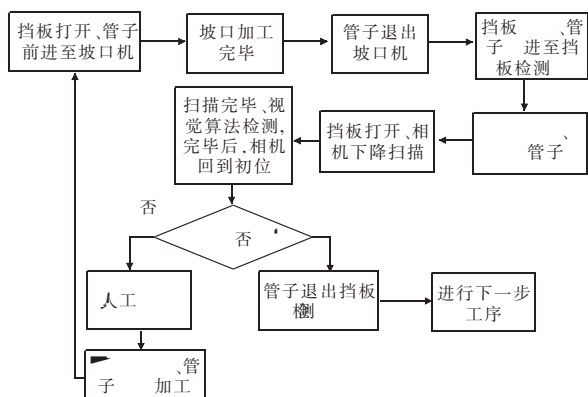
STEP2:

[5]

STEP3:



4

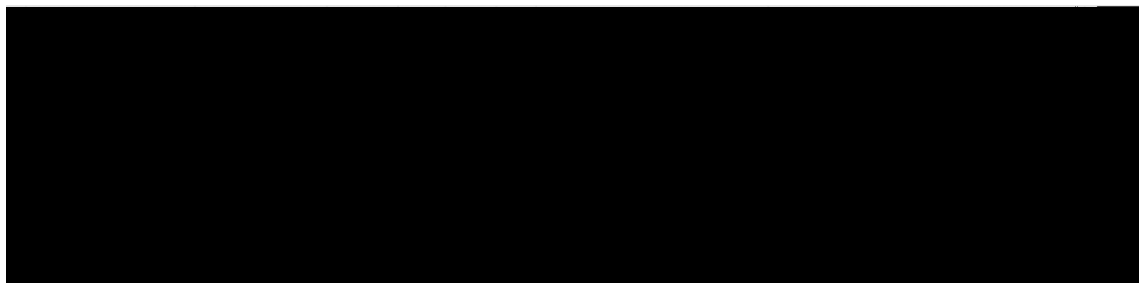


5

4

6

#	名称	数据类型	长度/精度	无符号的	允许 NUL	枚举	默认	注释	枚举类别	表达式
1	index	TINYINT	4	<input type="checkbox"/>	<input type="checkbox"/>	<input type="checkbox"/>	0	默认值0		
2	script_name	TEXT	65535	<input type="checkbox"/>	<input type="checkbox"/>	<input type="checkbox"/>		记录脚本名称		
3	server_name	TEXT	65535	<input type="checkbox"/>	<input type="checkbox"/>	<input type="checkbox"/>		记录服务器名称		
4	server_version	TINYINT	4	<input type="checkbox"/>	<input type="checkbox"/>	<input type="checkbox"/>		记录服务器版本		
5	server_version_comment	TEXT	65535	<input type="checkbox"/>	<input type="checkbox"/>	<input type="checkbox"/>		记录服务器版本注释		
6	protocol_version	TINYINT	4	<input type="checkbox"/>	<input type="checkbox"/>	<input type="checkbox"/>		记录协议版本		
7	connect_id	TINYINT	4	<input type="checkbox"/>	<input type="checkbox"/>	<input type="checkbox"/>		记录连接ID		
8	user	TEXT	65535	<input type="checkbox"/>	<input type="checkbox"/>	<input type="checkbox"/>		记录用户名		
9	host	TEXT	65535	<input type="checkbox"/>	<input type="checkbox"/>	<input type="checkbox"/>		记录主机名		
10	distance_between_encoder	SFLOAT	4	<input type="checkbox"/>	<input type="checkbox"/>	<input type="checkbox"/>		编码器之间的距离		
11	motor_scan_length	SMALLINT	6	<input type="checkbox"/>	<input type="checkbox"/>	<input type="checkbox"/>		扫描长度		
12	motor_scan_speed	SMALLINT	6	<input type="checkbox"/>	<input type="checkbox"/>	<input type="checkbox"/>		扫描速度		
13	motor_scan_timeout	SMALLINT	6	<input type="checkbox"/>	<input type="checkbox"/>	<input type="checkbox"/>		扫描超时		
14	outer_change_inspector	INT	11	<input type="checkbox"/>	<input type="checkbox"/>	<input type="checkbox"/>		刀具更换后的检测次数		
15	outer_change_inspector_detect	INT	11	<input type="checkbox"/>	<input type="checkbox"/>	<input type="checkbox"/>		刀具更换后的检测次数		
16	outer_change_inspector_detect_delay	INT	11	<input type="checkbox"/>	<input type="checkbox"/>	<input type="checkbox"/>		刀具更换后的检测延迟		
17	outer_change_inspector_detect_delay	INT	11	<input type="checkbox"/>	<input type="checkbox"/>	<input type="checkbox"/>		刀具更换后的检测延迟		



6

4

500

8 , , 0.15 mm,

、 , ○

、 ,

、 , ○

、 ,

○

5

:

[1] , , .  
[J]. ,2023(6):39-40+43

[2] , , , . [J].  
,2023(5):38-40

[3] , , , .  
[J]. ,2023,60(22):211-220

[4] , , , .  
[J]. ,2023,39(9):48-53

[5] , .  
[J]. ,2023,49(6):25-30

, SICK

,

○

,

东方电气

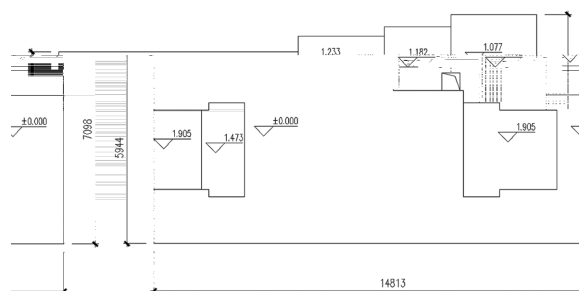


1

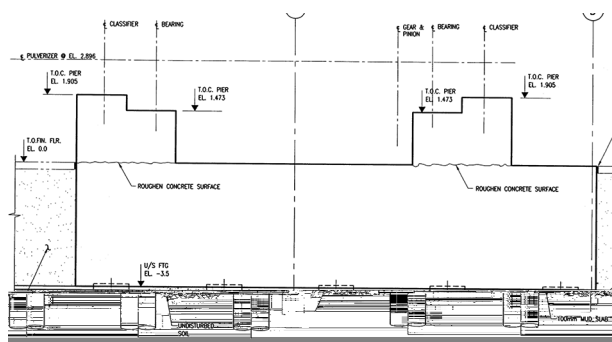
2×350 MW  
 , 2000  
 , 22 , ~1 100 kW,  
 ~480 kW, ~  
 18 t/h。

1.1

14 m, 6 m, -3.5 m,  
 1~2 -3.5 m。



1



2

1.2

2

110 mm

3



3

3

4

±0.000 m  
 350 mm , 12 2.3 m,  
 , 4 , 80 mm  
 , 5 , C80

±0.000 m

±0.000 m



(6) :

(7) :

,

(8) 80 mm ,

C80

(9) 0.000 m

(10)



10

(3) 300 mm

(4)

(5)

(6)

(7)

(8)

(9) 0.000 m

(10)

(11) 0.000 m

5.2

! !







m

。 、 ，

：

(1) ：

； ，

。

，

(2) ；LED

。 LED

，

(3) ； LED

， 、 ；

， (5 000~6 500 K)，

；

、 。

，

， 5 000 K ，  $\geq 0.9$   $\leq 90^\circ$

70 W~200 W LED ；

LED ， 120 lm/W， 200 W

LED 24 000 lm；70 W LED

8 400 lm

9

	1		
	LED	LED	
1 ( )	1	1	/
(W)	400	200	↓ 200
			70
(h)		12	/

(2)

:

(3)

:

[1]

:

[D].

,2020

[2]

[M].

:

,2016

[3]

[J].

2022(4):19-21

[4]

[J].

,2021,15(6):57-60

[5]

[J].

,2018(3):186-188

[6]

.F

[D].

,2021

[7]

[J].

( ),2003(1):30-32

[8]

[J].

,2011,

27(1):83-86

200

2025 2 18 ,

200

100

。

。

“

”

,

3 000

,

,

,

、

,

、

、

。

,

,

,

、

。

:

,

、

。

:

,

。

:

、

,

、

,

、

。

200

“

+

+

”

,

”

”

。

,

18

,

2018 ,

55

,

130

。

50

,

5

,

“

”

。

,

。

:

618000

： 、 、 ， 。  
、 、  
( DCS) ，DCS 。  
、 、 DCS 。 DCS - ， DCS  
、 、 。  
：D

：2024-12-16

： “ ” ： ( DCS) ； :2022JBZC005。

： (1988—)， ,2011

、 、 。

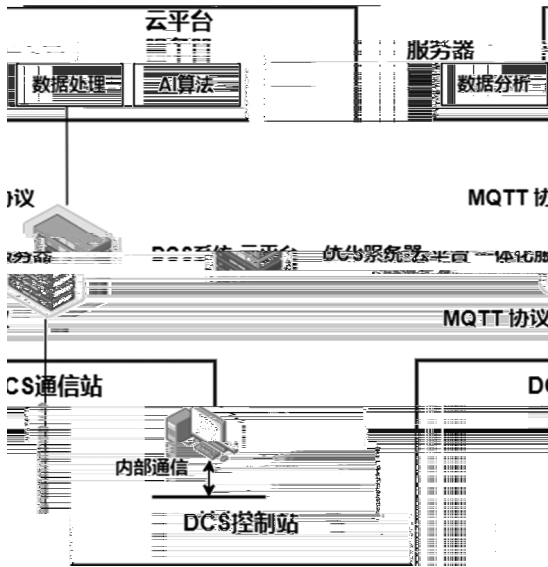


， ， ， DCS

。

，

1。



1 DCS

2

， ， DCS

， DCS

； DCS

， LED

， DCS DCS-

1。

1	DCS	DCS-
DCS		
DCS+	/	/

DCS-		DCS	DCS-
		2	
2	DCS	DCS-	

DCS	50 000 /	20 ms	10 000 /	50 ms
DCS+	100 000 /	5 ms	50 000 /	10 ms

DCS

， DCS-

DCS

43 %，

，

。

3

， DCS

， DCS

DCS

DCS -

， DCS

， DCS-

。

：

[1] ， ， . SCADA DCS [J]. ， 2023(2) ,7-10

[2] . DCS [D]. ， 2021

[3] ， ， ， . DCS SIS SCADA [J]. ， 2024(1) ,48-50

# PLC

618000

: , 0 \$ ! , ,  
o o ,  
,

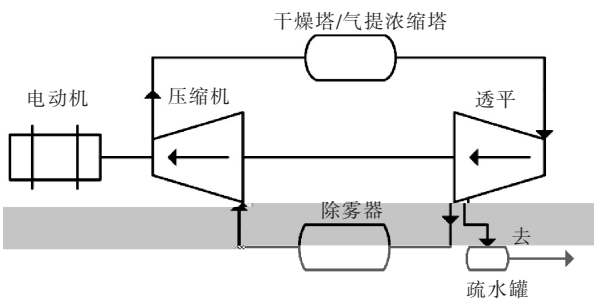
:2024-09-26

: (1984—), , , , ,  
,

(PLC)

PLC

1



1

2

PLC, (DCS), PC, PLC

:DCS

PC

PLC

PLC

PLC

LK PLC

PLC

LK PLC

LK PLC

LK PLC

PLC

3

LK411 PLC, LK511

LK430

PLC LK610

LK710

LK239

LK

HT

。 PLC  
、 PROFIBUS-DP

。 PLC 、 MODBUS  
TCP/IP 。  
2:

2

4

(1)

PLC

、 PLC

1。

1

1		PLC	
2		PLC	
3		PLC	
4	/	PLC	
5		PLC	,4~20 mA
6		TSI	PLC ,4~20 mA
7	X/Y	TSI	PLC ,4~20 mA
8		TSI	PLC ,4~20 mA
9	1X/1Y/2X/2Y	TSI	PLC ,4~20 mA
10			PLC PT100
11			PLC PT100
12			PLC ,4~20 mA
13			PLC PT100
14			PLC ,4~20 mA
15			PLC ,4~20 mA
16			PLC PT100
17			PLC ,4~20 mA
18			PLC PT100
19			PLC ,4~20 mA
20			PLC PT100
21			PLC ,4~20 mA

PLC

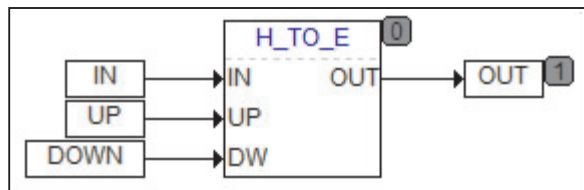
4

6

。 PLC

8  
Excel  
Excel  
Excel  
Excel  
, PLC  
(2)

4~20 mA  
0~20 mA,  
0~65535  
3



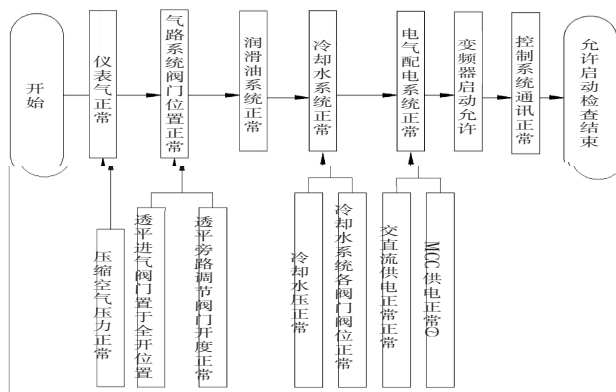
IN  
,UP  
,OUT  
( := \_ 04\_1, := 04\_1\_ ,  
:= 04\_1\_ , => \_ 04\_1);  
..... ( := \_ 04\_8, := 04\_8  
- , := 04\_8\_ , => \_ 04\_8);  
HTE ,IN ,UP DW  
,OUT  
1

Excel , Excel  
2 8

Excel

(3)

4。



4

PLC

(4)

+100 r/min -100 r/min

300 r/min, 1 000 r/min, 2 000 r/min

5。



5



# UPS

1 2

1. , 201309; 2. , 201108

: UPS , UPS 。  
 , , 。  
 , 。  
:UPS; ; ;  
:TM774 ;A :1001-9006(2025)02-0086-03

## Technology for Anti Override Trip Protect

:2024-09-25

: (1986—), ,2024

1.2

[3]

[4]

[5]

2

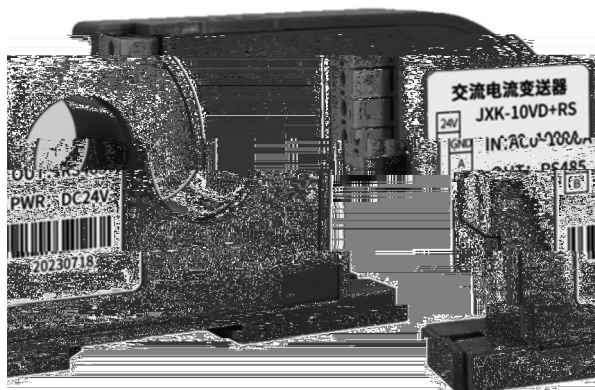
UPS

2.1

( 1)

[6]

RS485



1 RS485

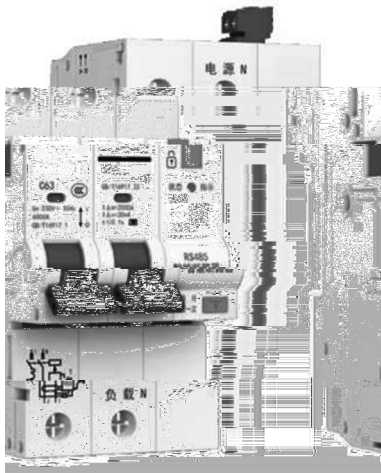
2.2

RS485

( 2),

RS485

[7]



2 RS485

2.3